

## Effect of initial $3\alpha$ cluster configurations in $^{12}\text{C}$ on the direct decay of its Hoyle state

Abhijit Baishya<sup>1,2,\*</sup>, S. Santra<sup>1,2,†</sup>, A. Pal,<sup>1</sup> and P. C. Rout<sup>1,2</sup>

<sup>1</sup>Nuclear Physics Division, Bhabha Atomic Research Centre, Mumbai 400085, India

<sup>2</sup>Homi Bhabha National Institute, Anushaktinagar, Mumbai 400094, India



(Received 8 March 2021; revised 12 May 2021; accepted 16 July 2021; published 2 August 2021)

We investigate the implications of initial  $3\alpha$  configurations in  $^{12}\text{C}$  corresponding to different decay modes of its Hoyle state on the penetrability ratios. Considering the second  $2^+$  (10.03 MeV) state to be a collective excitation of the Hoyle state, the direct  $3\alpha$  decay width for the Hoyle state has been calculated using the ratio of the barrier penetration probability of the Hoyle state to the  $2^+$  state. Semiclassical Wentzel–Kramers–Brillouin (WKB) approximation has been employed to determine the penetrability ratio, resulting in an upper limit on the branching ratio of the direct decay of the Hoyle state in “equal phase-space” (DD $\phi$ ) mode as  $\frac{\Gamma_{3\alpha}}{\Gamma} < 3.1 \times 10^{-6}$ . However, this limit for “linear chain” (DDL) decay is  $\frac{\Gamma_{3\alpha}}{\Gamma} < 2.6 \times 10^{-7}$ , which is one order of magnitude smaller than the DD $\phi$  decay and the limit for “equal energy” (DDE) decay is  $\frac{\Gamma_{3\alpha}}{\Gamma} < 1.5 \times 10^{-5}$ , which is greater than both DD $\phi$  and DDL decays. It implies that the limit on direct decay probability is strongly dependent on the initial configuration of the  $3\alpha$  cluster. A further probe using a bent-arm-like  $3\alpha$  initial configuration shows that the direct decay probability is maximum when the angle of the bent arm is  $\approx 120^\circ$ , an important ingredient for understanding the Hoyle-state structure.

DOI: [10.1103/PhysRevC.104.024601](https://doi.org/10.1103/PhysRevC.104.024601)

### I. INTRODUCTION

The study of Hoyle state of  $^{12}\text{C}$  at 7.65 MeV is a topic of continued interest because of its importance in describing the  $^{12}\text{C}$  abundance in our universe. The structure and decay properties of the Hoyle state play key roles in the stellar nuclear synthesis. In the helium-burning phase of stars,  $^{12}\text{C}$  is produced through a  $3\alpha$  capture process in which first two  $\alpha$  particles are fused to produce  $^8\text{Be}$  which further captures another  $\alpha$  to form a  $^{12}\text{C}$ . This capture when proceeded via  $s$ -wave resonance can boost the carbon production by a factor of 10–100 million [1]. To explain the abundance of  $^{12}\text{C}$ , Hoyle predicted a resonant state near 7.65 MeV, just above the  $3\alpha$  breakup threshold of  $^{12}\text{C}$  (7.27 MeV) [1], and subsequently its existence was confirmed experimentally [2,3].

There are ambiguities with respect to the structure of the Hoyle state where different theories have come up with different answers. Algebraic cluster model predicts the Hoyle state to be an equilateral triangle made up of  $3\alpha$  [4]. Antisymmetrized molecular dynamics and fermionic molecular dynamics calculations predict a triangular  $^8\text{Be} + \alpha$  configuration [5,6]. There is also a Bose-Einstein condensation theory which extends the idea of happening condensation in molecular systems to a nuclear system, which suggests if the  $3\alpha$  density is low, it can show condensation [7,8]. Recently *ab initio* nuclear lattice simulations using chiral effective field theory [9,10] has concluded that the Hoyle state may have a bent-arm-like structure. All these models have successfully

reproduced various observational parameters of the Hoyle state. Using Faddeev equations in a  $3\alpha$  continuum it has been shown [11,12] that the change in structure from small to large distances from the decay of the Hoyle state is very small, and therefore the final state distribution in this case indeed can be taken as a rather direct probe of its  $\alpha$ -cluster structure.

Raduta *et al.* [13] argue that a linear chain structure of the Hoyle-state should result in the center of the three  $\alpha$  particles to be at rest and the other two sharing the total energy equally get emitted in opposite direction along the linear chain (DDL mode), while a “Bose-Einstein condensate” structure of the Hoyle state should decay into three equal energy  $\alpha$  particles emitted at an angle of  $120^\circ$  relative to each other (DDE mode). However, in DD $\phi$  (decay in equal phase-space) mode, the three  $\alpha$  particles are emitted in such a way that they fill the entire phase space available to them. Schematic representations of the initial  $3\alpha$  cluster configurations corresponding to the above three direct decay modes are shown in Fig. 1.

In recent years, quite a few experiments have been performed to quantify this direct decay component of the Hoyle state which is supposed to throw new light on the structure. An upper limit of 0.019% was put by T. Rana *et al.* [14] which is actually the upper limit of DD $\phi$  decay, for DDL decay they put an upper limit of 0.004% and for DDE decay the same is 0.012%.

Although the Hoyle state is at the center of all attention, quite fascinating is the second  $2^+$  (10.03-MeV) state [15] which is believed to be a collective excitation of the Hoyle state itself which is also supported by the observation of a rotational band and reduced  $\alpha$  decay width [4,16]. This implies that we can infer features of Hoyle state by observing the  $2^+$  state alternatively. For example, by observing the direct decay

\*abaishya@barc.gov.in

†ssantra@barc.gov.in

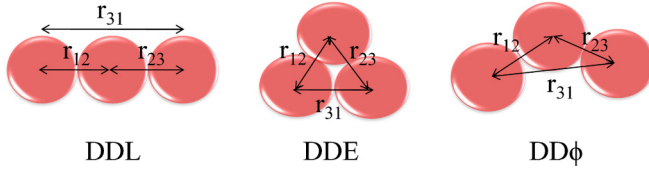


FIG. 1. Initial  $3\alpha$  cluster configurations for direct decay modes in linear chain (DDL), equal energy (DDE), and equal phase space (DD $\phi$ ).

component of the  $2^+$  state we can find out information about the direct decay component of the Hoyle state.

More recently, R. Smith *et al.* [11] have given an upper limit of the direct decay branch invoking  $R$ -matrix properties of the  $2^+$  state and concluded that  $\frac{\Gamma_{3\alpha}}{\Gamma} < 5.7 \times 10^{-6}$  for DD $\phi$  but did not take into account the initial configuration of the  $3\alpha$  cluster, which as suggested before carries the signature of the structure. In the present work, we have done a detailed analysis following a similar approach and also two additional approaches leading to very different results as described below.

## II. ANALYSIS FRAMEWORK

The present analysis is built around the framework adopted by Smith *et al.* [11] though with a few important modifications. Monte Carlo simulation has been performed to find out the barrier penetrability ratio of the direct decay of Hoyle state to the direct decay of  $2^+$  state. The  $2^+$  state can undergo decay into  $3\alpha$  in three different ways: (i) sequential decay through  $\alpha + {}^8\text{Be}_{g.s.}$ , (ii) sequential decay through  $\alpha + {}^8\text{Be}_{2^+}$ , and (iii) direct decay into  $3\alpha$ . The first decay channel which contributes more than 98% of the total decay of  $2^+$  have been clearly identified by Zimmerman *et al.* [15]. So the remaining contribution which is less than 2% comes from the second and third channels. The total decay width, obtained from  $R$ -matrix fit to the experimental decay data, is 1.60(13) MeV [17]. Thus, the sum of the decay widths of the other two  $\alpha$  decay channels (which could not be separated experimentally) will be equal to  $\approx 32$  (4) keV. Hence, the decay width of only the direct decay will have an upper limit of 32 keV, i.e.,  $\Gamma_{3\alpha}^{2^+} < 32$  keV, the information which is used as an input to the present simulation.

According to the  $R$ -matrix theory [18,19] the partial width of a state is given by

$$\Gamma_i = 2P_i\gamma_i^2, \quad (1)$$

where  $P_i$  is the penetrability factor and  $\gamma_i^2$  is the reduced channel width. The ratio of reduced channel width to Wigner limit is given by  $\theta_i^2$  and defined as

$$\gamma_i^2 = \theta_i^2 \frac{3}{2} \frac{\hbar^2}{MR^2}. \quad (2)$$

Since the  $2^+$  state is considered to be a collective excitation of the Hoyle state [20], one can assume that,  $\theta_{\text{DD}}^2(\text{Hoyle}) = \theta_{\text{DD}}^2(2^+)$ , implying  $\gamma_{\text{DD}}^2(\text{Hoyle}) = \gamma_{\text{DD}}^2(2^+)$ .

Combining the above equality with Eq. (1), one can obtain

$$\Gamma_{\text{DD}}(\text{Hoyle}) = \Gamma_{\text{DD}}(2^+) \frac{P_{\text{DD}}(\text{Hoyle})}{P_{\text{DD}}(2^+)}. \quad (3)$$

The decay dynamics of  ${}^{12}\text{C}$  into three  $\alpha$  particles can be described by following the hyperspherical coordinate formalism [21,22], where one can express the Coulomb, centrifugal and nuclear potentials of the three-body system as functions of the hyper-radius “ $\rho$ ” of the system which is given by [21]

$$\rho^2 \equiv \frac{1}{mM} \sum_{i<k} m_i m_k \mathbf{r}_{ik}^2, \quad \mathbf{r}_{ik}^2 = (\mathbf{r}_i - \mathbf{r}_k)^2, \quad (4)$$

where  $M = \sum m_i$  and  $m$  is an arbitrary normalization mass.

The probability of decay can be calculated by the Wentzel–Kramers–Brillouin (WKB) approximation for a hyper-radial potential as

$$T = \frac{1}{1 + \exp(2S)} \quad (5)$$

and  $S$  is given by

$$S = \frac{1}{\hbar} \int_{\rho_1}^{\rho_2} d\rho \sqrt{2m[V(\rho) - E]}, \quad (6)$$

where  $E$  is the kinetic energy of the particles after separation and  $\rho_{1,2}$  are the classical turning points with  $V(\rho_{1,2}) = E$ . The total potential  $V(\rho)$  consists of Coulomb, centrifugal, and nuclear terms.

The Coulomb potential in terms of the scaling factors ( $s_{ik}$ ) is expressed as

$$V_{\text{Coulomb}}(\rho) = \sum_{i<k} \frac{Z_i Z_k e^2}{r_{ik}} = \frac{1}{\rho} \sum_{i<k} \frac{Z_i Z_k e^2}{s_{ik}}, \quad (7)$$

where

$$s_{ik}^2 = \frac{\mathbf{r}_{ik}^2}{\rho^2}. \quad (8)$$

The values of  $s_{ik}$  and  $\rho_0$  (the hyper-radius corresponding to the initial configuration of the system) are different for different modes. For a particular mode, the  $r_{ik}$  values can be obtained from initial configurations shown in Fig. 1 and used in Eq. (4) to determine  $\rho$  which in turn used in Eq. (8) to determine  $s_{ik}$ . These scaling factors,  $s_{ik}$ , determine the decay path and remain constant throughout [21].

The centrifugal potential takes the form as

$$V_{\text{Centrifugal}}(\rho) = \frac{\hbar^2(K + 3/2)(K + 5/2)}{2m\rho^2}, \quad (9)$$

where  $K$  is the hypermomentum of the system. For direct decay, the lowest value of hypermomentum is given by  $K_{\text{min}} = l_{12,3} + l_{12}$ , where  $l_{12,3}$  and  $l_{12}$  correspond to the angular momentum associated with the relative two-body motion of the decay particles. For the present study, the value of  $K$  is taken to be “zero” for the Hoyle state and “2” for the first excited state of the Hoyle state.

The nuclear potential is considered to be of Woods-Saxon volume form with parameters taken from Ref. [23]. The total potential  $V$  consisting of Coulomb ( $V_C$ ) and centrifugal ( $V_l$ ) terms and then with additional nuclear term ( $V_N$ ) calculated for DDL and DDE decay modes independently are shown in Fig. 2(a). The presence of centrifugal term increases the barrier height for  $2^+$  state as shown in Fig. 2(b). No potential is shown for DD $\phi$  mode as it does not correspond to a single

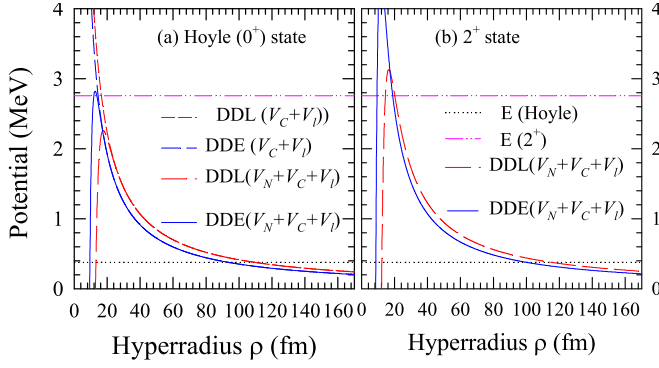


FIG. 2. Sum of the Coulomb ( $V_C$ ) and centrifugal potentials ( $V_l$ ) with and without the nuclear term ( $V_N$ ) for DDL and DDE modes of direct decay. Dotted and dot-dot-dashed horizontal lines represent the energies of Hoyle state and  $2^+$  state above the  $3\alpha$  breakup threshold correspond to 0.38 and 2.756 MeV, respectively.

structure. From Fig. 2, one can find that the potentials corresponding to two decay modes are not identical and giving rise to different values of  $\rho_1$  and  $\rho_2$ .

With the available code “PETA” [24], one can obtain only the decay width for the  $DD\phi$  mode, i.e., the decay in equal phase space where three  $\alpha$  particles are emitted in such a way that they fill the entire phase space available to them. But the direct decay is known to have other possible decay modes like DDL and DDE. In order to describe all the above three decay modes a new Monte Carlo code “BPP” based on FORTRAN language has been developed recently [25], which is an enhanced version of “PETA.” The important characteristics of this code is that it includes the effect of initial configuration on barrier penetrability and has a much improved phase-space sampling algorithm for better consistency. It also has the provision of including the nuclear interaction in addition to Coulomb and centrifugal terms. The code samples the kinematically available phase space for the three-body system and calculates the barrier penetration probability using the Eqs. (4)–(9). The new “BPP” code has been used to obtain the barrier penetration probabilities which interestingly are found to be substantially different for different decay modes. Importantly, the ratios of penetrabilities of the Hoyle state to  $2^+$  state for DDL, DDE, and  $DD\phi$  decay modes and their respective decay widths, as given in Table I, have also been found to be very different. Due to the uncertainties in the nuclear potential, an error on the above ratios has been estimated to be  $\approx 10\%$ . The large variation in the above ratios observed from one mode of decay to the other indicates the importance of the role played by the initial configuration of  $^{12}\text{C}$ .

From Fig. 2, we see that the addition of nuclear term modifies the Coulomb+centrifugal potential only at  $\rho < 15$  fm and  $\rho_1$  is very close to  $\rho_0$ . So one can simplify the above calculations by neglecting the nuclear term and replacing  $\rho_1$  by  $\rho_0$ . The uncertainties created due to the exclusion of nuclear potential can be simulated by calculating the barrier penetration probabilities for different values of  $\rho_0$  with radius parameter  $r_0$  (in the range of 0.85–1.60 fm), where the radius  $R = r_0 A^{1/3}$  with  $A = 4$  being the atomic mass number of  $\alpha$ . The experimental value of  $r_0$  for  $\alpha$  is 1.05 fm [26], however,

TABLE I. Ratio of “Penetrability” and “Width” for different decay modes using the  $3\alpha$  interaction including and excluding the nuclear term, obtained from the “first approach.”

Decay modes	$\frac{P_{DD}(\text{Hoyle})}{P_{DD}(2^+)}$	$\frac{\Gamma_{DD}(\text{Hoyle})}{\Gamma(\text{Hoyle})}$
	$(V = V_C + V_l + V_N)$	
$DD\phi$	$(1.5 \pm 0.2) \times 10^{-11}$	$< 5.7 \times 10^{-8}$
DDL	$(3.2 \pm 0.3) \times 10^{-11}$	$< 1.2 \times 10^{-7}$
DDE	$(2.1 \pm 0.2) \times 10^{-9}$	$< 7.8 \times 10^{-6}$
	$(V = V_C + V_l)$	
$DD\phi$	$(4.8 - 7.3) \times 10^{-10}$	$< 3.1 \times 10^{-6}$
DDL	$(2.9 - 6.2) \times 10^{-11}$	$< 2.6 \times 10^{-7}$
DDE	$(2.1 - 3.6) \times 10^{-9}$	$< 1.5 \times 10^{-5}$

an  $R$ -matrix fit to the  $2^+$  resonance curve measured using the  $^{12}\text{C}(\gamma, \alpha_0)^8\text{Be}(\text{g.s.})$  reaction provides a large value of  $r_0 = 1.60$  fm [17] hinting at an extended structure. Though the penetration probability is highly sensitive to the radius parameter  $r_0$ , the ratio of the penetrability for any particular mode of decay is not so sensitive. The results on the probability ratios of individual decay modes obtained for  $r_0$  in the range of 0.85–1.60 fm have been listed in the lower half of Table I which are in close agreement with the ones obtained from the potential including nuclear term. Most importantly, the huge difference found in the penetrability ratios for different decay modes obtained using either of the two potentials confirms the dependence of direct decay probabilities on the initial  $3\alpha$  configuration inside  $^{12}\text{C}$ .

Using Eq. (3) and the known width of the Hoyle state,  $\Gamma(\text{Hoyle}) = 8.5(1)$  eV, one can obtain the upper limits on the branching ratios for different direct decay modes. The upper limits for  $DD\phi$ , DDL, and DDE modes of breakup, using  $V = V_C + V_l$ , are found to be  $3.1 \times 10^{-6}$ ,  $2.6 \times 10^{-7}$ , and  $1.5 \times 10^{-5}$ , respectively. It is quite clear that the ratio varies quite substantially depending on the mode of breakup. So it is very crucial to mention the mode of breakup before giving any upper limit for the branching ratio. This seems to be due to the consideration of initial structure for various phase-space points. Also, the value on the upper limit for  $DD\phi$  decay is found to be smaller than what is reported by Smith *et al.* [11] where a single initial structure for all the phase-space points has been considered. It may be noted that the above limits may slightly increase by a common factor of 1.33 if  $\theta_{\alpha_0}^2$  for  $0^+$  and  $2^+$  states are unequal and considered to be 2.0 and 1.5, respectively, as given in Refs. [27–29].

### A. Second approach

A “second approach,” similar to that of Zheng *et al.* [30], has also been employed to compute the ratio of the  $\Gamma$  width, which is conceptually not too different from the one discussed so far, but provides different results. In this approach, it is assumed that the reduced decay width for the direct decay of Hoyle state and its sequential decay are equal. Using Eq. (1), one can obtain the ratio of the decay widths of the two modes to be equal to the ratio of their respective barrier penetration probabilities. Recalling Eq. (4), one can assume

TABLE II. Branching ratios for different direct decay modes of the Hoyle state obtained from the “second approach” using the potential with and without nuclear term.

Decay Modes	$\frac{\Gamma_{DD}}{\Gamma} (\approx \frac{P_{DD}}{P_{Seq.}})$	$\frac{\Gamma_{DD}}{\Gamma} (\approx \frac{P_{DD}}{P_{Seq.}})$
	$(V = V_C + V_I + V_N)$	$(V = V_C + V_I)$
DD $\phi$	$(6.2 \pm 0.6) \times 10^{-7}$	$(0.41-5.06) \times 10^{-7}$
DDL	$(1.6 \pm 0.2) \times 10^{-7}$	$(0.33-6.83) \times 10^{-8}$
DDE	$(1.4 \pm 0.1) \times 10^{-6}$	$(0.41-4.47) \times 10^{-6}$

$\theta_{DD}^2(\text{Hoyle}) = \theta_{Seq.}^2(\text{Hoyle})$ , and hence,

$$\gamma_{DD}^2(\text{Hoyle}) = \gamma_{Seq.}^2(\text{Hoyle}), \quad (10)$$

which leads to

$$\frac{\Gamma_{DD}(\text{Hoyle})}{\Gamma_{Seq.}(\text{Hoyle})} = \frac{P_{DD}(\text{Hoyle})}{P_{Seq.}(\text{Hoyle})}. \quad (11)$$

Since,  $\Gamma_{Seq.}(\text{Hoyle}) \approx \Gamma(\text{Hoyle})$ , we have

$$\frac{\Gamma_{DD}(\text{Hoyle})}{\Gamma(\text{Hoyle})} \approx \frac{P_{DD}(\text{Hoyle})}{P_{Seq.}(\text{Hoyle})}. \quad (12)$$

So the branching ratio for the direct decay is equal to the penetrability ratio of direct decay to the sequential decay. Using a different module of the BPP code [25], the penetrabilities for the sequential decay have been calculated using the interaction with and without the nuclear term [31]. The values of the penetrability ratios or the branching ratios with uncertainties thus obtained are listed in Table II. The results show that the branching ratios for all the three decay modes are slightly different from those obtained from the “first approach.” So, accordingly, one gets different values of upper bounds compared to the “first approach.” The reason for this discrepancy between the two approaches may be due to the assumption regarding the reduced width. However, a deeper understanding of the  $R$ -matrix theory in conjunction with the reduced width of the cluster states is essential to establish the effectiveness of either approach.

### B. Third approach

Finally, a “third approach” is considered in which we explore the conclusions given by Epelbaum *et al.* [10], where the Hoyle state has been assumed to have a bent-arm-like structure. However, in the present work, the angle of the bent arm has been kept as a variable and the simulations made for angles in the range of 0–180°. Separate calculations have been performed using each of the formalisms of the above two techniques. Barrier penetration probabilities for direct decay are calculated assuming the bent-arm structure for both Hoyle state as well as its  $2^+$  state. Using Eq. (3), the branching ratio is obtained as a function of angle of bent arm as shown in Fig. 3(a). A maximum observed at  $\approx 120^\circ$  implies that the branching ratio of the direct to total decay is the highest when the angle of the bent arm is  $120^\circ$ . Whether this configuration is favored or not is a question and raises some debate

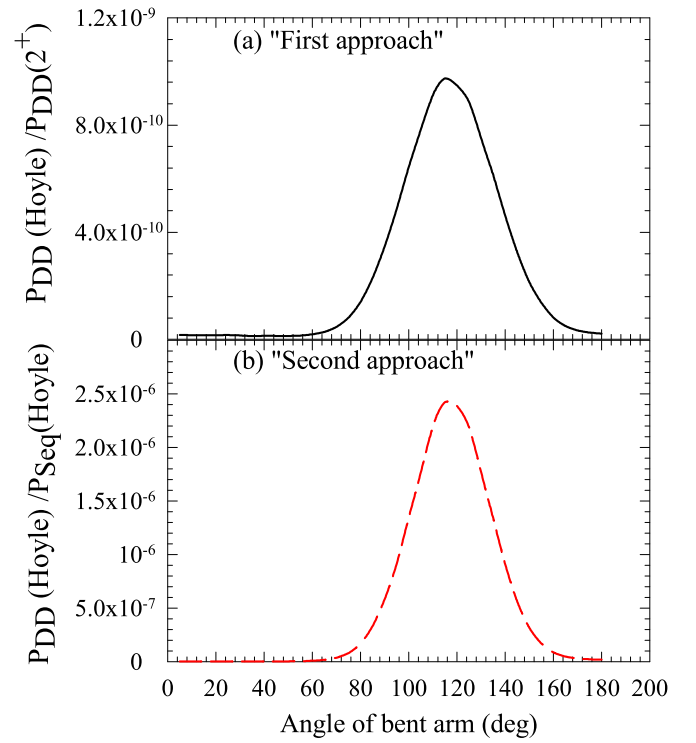


FIG. 3. Penetrability ratio as a function of the angle of the bent arm (a)  $P_{DD}^{\text{bent-arm}}(\text{Hoyle})/P_{DD}^{\text{bent-arm}}(2^+)$  from “first approach” (b)  $P_{DD}^{\text{bent-arm}}(\text{Hoyle})/P_{Seq.}^{\text{bent-arm}}(\text{Hoyle})$  from “second approach.”

but it clearly differs from the results obtained by Epelbaum *et al.* [10].

The calculation is repeated following the “second approach,” where one calculates the penetrability for a sequential decay considering the bent-arm structure and again finds out the branching ratio as a function of the angle of bent arm using Eq. (12), as shown in Fig. 3(b). A maximum around  $120^\circ$ , the result similar to the one obtained from the first technique, has been observed. The results look very interesting because, for both the approaches (“first” and “second”) considered, a maximum is observed in the branching ratio at around  $120^\circ$  meaning the structure to be a obtuse angled triangle. What this actually means is not clear yet; however, this may give some idea regarding possible  $\alpha$  configuration inside the Hoyle state when compared with measured direct decay components.

In a recent observation by J. Bishop *et al.* [32], a 95% confidence belt of upper and lower limit was formed. Accordingly, the direct decay component has a upper limit 0.043% and a lower limit of 0.0058%. But to extract the direct decay component, a more realistic model (DDP<sup>2</sup>) [32] was considered later instead of a simple phenomenological one. This model considers direct decay in entire phase space but weighted by penetrability. The present work using DDP<sup>2</sup> model and “first approach” gives an upper limit of (0.019–0.028)%. This result lies within the experimental limit quoted by [32]. Also, the “second approach” provides an absolute value for DDP<sup>2</sup> branching ratio in the range of (0.01–0.035)% corresponding to  $r_0 = 1.05-1.60$  fm. It is interesting to note that the

branching ratio calculated at  $r_0 = 1.6$  fm reproduces the experimental value (0.035%) observed by Smith *et al.* [33] and is also within the experimental confidence belt obtained by Bishop *et al.* [32].

It is seen from the present work that the phase-space points close to DDE are more favorable in terms of penetrability and in the case of DDP<sup>2</sup>, the major contribution comes from these points. This implicates that DDE mode may be the most prominent decay mode after all. Instead of a single point in the phase space, DDE may occupy a zone around this point due to inherent quantum mechanical uncertainties and perturbations and can explain why this mode is the major contributor in the DDP<sup>2</sup>.

### C. Simulated spectrum

Next, we try to see the implications of very low branching ratios in a real experiment. As seen from the results of all three approaches, we find that out of all the approaches considered for simulation, in the best-case scenario one can have a branching ratio of around  $10^{-5}$  which is still 5 times lower than what was achieved by Rana *et al.* [14]. Such low branching ratios mean that one needs very long and high statistics experiment to get a significant number of direct decay events. In order to simulate what happens if we do perform such a high statistics experiment, we perform a Monte Carlo simulation which generates the events for various direct decay modes and then mix these different decay events according to our current knowledge of the branching ratio [14]. The spectra obtained from the simulations are shown in Fig. 4 with gray, red, pink, and yellow regions representing the sequential, DDL, DDE, and DD $\phi$  decay events. The blue star symbols represent the sum of all the contributions and are supposed to imitate the data events obtained from a real experiment. It may be emphasized that the energy and angular resolutions of the detectors have been considered to be 40 keV and  $0.3^\circ$ , respectively, to build these spectra.

Now we have to find out whether we can reliably extract back the branching ratio information from the above combined spectrum which replicates an experimental data. This will help us plan any future experiment for measuring the direct decay branching more effectively. The conventional fitting procedure (ROOT TFractionFitter) is employed to fit a typical combined data described above and the results are shown in Fig. 4. The plot shows a successful fitting for a branching ratio of  $2 \times 10^{-4}$ . It is interesting to find that a branching ratio of less than  $\approx 10^{-4}$  cannot be fitted reliably without having a very large statistics which also raises the issue of computational limitation.

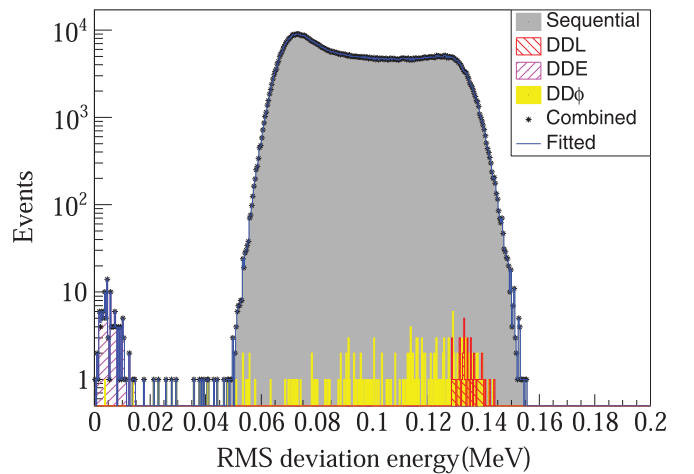


FIG. 4. Simulated root-mean-square energy deviation spectrum of three  $\alpha$  particles emitted via different decay modes, with dominant contribution (99.965%) from sequential mode as shown by gray shade. Contribution from DDL, DDE, and DD $\phi$  modes are 0.004%, 0.012%, and 0.019% respectively. Combined events shown by blue solid line have been fitted again to find the uncertainty in extracting back the above contributions if possible.

### III. CONCLUSIONS

In summary, using elaborate simulations, it has been found that the dependence of penetrability on the initial configuration of three  $\alpha$  inside  $^{12}\text{C}$  is quite sensitive. It may be concluded that it is necessary to specify the initial configuration, which is very important, while mentioning any upper limit for direct decay branching ratio. For the first time, we make use of a different approach to calculate the branching ratio and we find that this method further reduces its limit. However, this technique should in principle give an absolute branching ratio instead of an upper limit. We also explore the specific case where Hoyle state is assumed to have a bent-arm-like structure and the results obtained by varying the angle of the bent arm are found to be quite interesting. Last, we simulate a real life like experiment where we mix the events of direct decay modes with the sequential mode in proportion to their respective branching ratios known so far and try to find out whether our current minimization techniques are able to extract the specific mixing ratios. We find that the techniques are not sensitive enough below the branching ratio of  $\approx 10^{-4}$  even when using a reasonably large sample volume for the Monte Carlo simulation. Present results will not only serve as important inputs to the future measurements but also open up further simulations and theoretical work on the study of direct decay of the Hoyle state.

- [1] F. Hoyle, *Astrophys. J., Suppl. Ser.* **1**, 121 (1954).
- [2] D. Dunbar, R. Pixley, W. Wenzel, and W. Whaling, *Phys. Rev.* **92**, 649 (1953).
- [3] C. Cook, W. Fowler, C. Lauritsen, and T. Lane, *Phys. Rev.* **107**, 508 (1957).
- [4] R. Bijker and F. Iachello, *Ann. Phys. (NY)* **298**, 334 (2002).

- [5] Y. Kanada-Enyo, *Prog. Theor. Phys.* **117**, 655 (2007).
- [6] M. Chernykh, H. Feldmeier, T. Neff, P. von Neumann-Cosel, and A. Richter, *Phys. Rev. Lett.* **98**, 032501 (2007).
- [7] A. Tohsaki, H. Horiuchi, P. Schuck, and G. Röpke, *Phys. Rev. Lett.* **87**, 192501 (2001).

- [8] Y. Funaki, H. Horiuchi, W. von Oertzen, G. Ropke, P. Schuck, A. Tohsaki, and T. Yamada, *Phys. Rev. C* **80**, 064326 (2009).
- [9] E. Epelbaum, H. Krebs, D. Lee, and Ulf-G. Meissner, *Phys. Rev. Lett.* **106**, 192501 (2011).
- [10] E. Epelbaum, H. Krebs, T. A. Lähde, D. Lee, and Ulf-G. Meißner, *Phys. Rev. Lett.* **109**, 252501 (2012).
- [11] R. Smith, M. Gai, M. W. Ahmed, M. Freer, H. O. U. Fynbo, D. Schweitzer, and S. R. Stern, *Phys. Rev. C* **101**, 021302(R) (2020).
- [12] M. Freer and H. Fynbo, *Prog. Part. Nucl. Phys.* **78**, 1 (2014).
- [13] A. Raduta, B. Borderie, E. Geraci, N. Le Neindre, P. Napolitani, M. Rivet, R. Alba, F. Amorini, G. Cardella, M. Chatterjee *et al.*, *Phys. Lett. B* **705**, 65 (2011).
- [14] T. Rana, S. Bhattacharya, C. Bhattacharya, S. Manna, S. Kundu, K. Banerjee, R. Pandey, P. Roy, A. Dhal, G. Mukherjee *et al.*, *Phys. Lett. B* **793**, 130 (2019).
- [15] W. R. Zimmerman, M. W. Ahmed, B. Bromberger, S. C. Stave, A. Breskin, V. Dangendorf, T. Delbar, M. Gai, S. S. Henshaw, J. M. Mueller, C. Sun, K. Tittelmeier, H. R. Weller, and Y. K. Wu, *Phys. Rev. Lett.* **110**, 152502 (2013).
- [16] M. Freer, H. Fujita, Z. Buthelezi, J. Carter, R. W. Fearick, S. V. Förtsch, R. Neveling, S. M. Perez, P. Papka, F. D. Smit, J. A. Swartz, and J. A. Usman, *Phys. Rev. C* **80**, 041303(R) (2009).
- [17] M. Freer, H. Horiuchi, Y. Kanada-En'yo, D. Lee, and Ulf-G. Meißner, *Rev. Mod. Phys.* **90**, 035004 (2018).
- [18] P. Descouvemont and D. Baye, *Rep. Prog. Phys.* **73**, 036301 (2010).
- [19] M. Lane and R. G. Thomas, *Rev. Mod. Phys.* **30**, 257 (1958).
- [20] H. Morinaga, *Phys. Rev.* **101**, 254 (1956).
- [21] E. Garrido, D. V. Fedorov, A. S. Jensen, and H. O. U. Fynbo, *Nucl. Phys. A* **748**, 27 (2005).
- [22] E. Nielsen, D. V. Fedorov, A. S. Jensen, and E. Garrido, *Phys. Rep.* **347**, 373 (2001).
- [23] L. Marquez, *Phys. Rev. C* **28**, 2525 (1983).
- [24] R. Smith, Peta version 1.0, matlab file exchange, 70496 (2019), <https://www.mathworks.com/matlabcentral/fileexchange/70496-peta-penetrability-of-three-alphas>.
- [25] A. Baishya, Barrier penetration probability using wkb technique, github (2021), <https://github.com/abhijitb498/BPP>.
- [26] J. J. Krauth, K. Schuhmann, M. A. Ahmed *et al.*, *Nature (Lond.)* **589**, 527 (2021).
- [27] V. V. Balashov and I. Rotter, *Nucl. Phys.* **61**, 138 (1965).
- [28] C. W. Cook, W. A. Fowler, C. C. Lauritsen, and T. Lauritsen, *Phys. Rev.* **111**, 567 (1958).
- [29] Y. Suzuki, H. Horiuchi, and K. Ikeda, *Prog. Theor. Phys.* **47**, 1517 (1972).
- [30] H. Zheng, A. Bonasera, M. Huang, and S. Zhang, *Phys. Lett. B* **779**, 460 (2018).
- [31] D. C. Cuong, P. Descouvemont, D. T. Khoa, and N. H. Phuc, *Phys. Rev. C* **102**, 024622 (2020).
- [32] J. Bishop, G. V. Rogachev, S. Ahn, E. Aboud, M. Barbui, A. Bosh, C. Hunt, H. Jayatissa, E. Koshchiy, R. Malecek *et al.*, *Phys. Rev. C* **102**, 041303(R) (2020).
- [33] R. Smith, J. Bishop, C. Wheldon, and T. Kokalova, *J. Phys.: Conf. Ser.* **1308**, 012021 (2019).